New Phytologist

Gross and net production during the spring bloom along the Western Antarctic Peninsula

Johanna A. L. Goldman[1], Sven A. Kranz[1], Jodi N. Young[1], Philippe D. Tortell[2], Rachel H. R. Stanley[3], Michael L. Bender[1] and Francois M. M. Morel[1]

[1]Department of Geosciences, Princeton University, Princeton, NJ 08544, USA; [2]Department of Earth, Ocean and Atmospheric Sciences, Department of Botany, University of British Columbia, Vancouver, BC V6T 1Z4, Canada; [3]Department of Marine Chemistry and Geochemistry, Woods Hole Oceanographic Institution, Woods Hole, MA 02543-1050, USA

Author for correspondence:
Johanna A. L. Goldman
Tel: +1 609 258 2612
Email: johannag@princeton.edu

Received: *18 March 2014*
Accepted: *15 September 2014*

New Phytologist (2015) **205:** 182–191
doi: 10.1111/nph.13125

Key words: cold adaptation, cyclic electron flow (CEF), *Fragilariopsis cylindrus*, gross production, net community production, respiration, Western Antarctic Peninsula.

Summary

- This study explores some of the physiological mechanisms responsible for high productivity near the shelf in the Western Antarctic Peninsula despite a short growing season and cold temperature.
- We measured gross and net primary production at Palmer Station during the summer of 2012/2013 via three different techniques: incubation with $H_2{}^{18}O$; incubation with $^{14}CO_2$; and *in situ* measurements of O_2/Ar and triple oxygen isotope. Additional laboratory experiments were performed with the psychrophilic diatom *Fragilariopsis cylindrus*.
- During the spring bloom, which accounted for more than half of the seasonal gross production at Palmer Station, the ratio of net-to-gross production reached a maximum greater than *c*. 60%, among the highest ever reported. The use of multiple techniques showed that these high ratios resulted from low heterotrophic respiration and very low daylight autotrophic respiration. Laboratory experiments revealed a similar ratio of net-to-gross O_2 production in *F. cylindrus* and provided the first experimental evidence for an important level of cyclic electron flow (CEF) in this organism.
- The low ratio of community respiration to gross primary production observed during the bloom at Palmer Station may be characteristic of high latitude coastal ecosystems and partially supported by a very active CEF in psychrophilic phytoplankton.

Introduction

The Western Antarctic Peninsula (WAP) is among the most productive regions in the Southern Ocean (Arrigo *et al.*, 2008a,b), where spring phytoplankton blooms result in a large Net Community Production (NCP = photosynthesis minus respiration) supporting an abundant and diverse ecosystem (Ducklow *et al.*, 2007). Over the past several decades, the WAP has also experienced some of the most extreme atmospheric warming on the planet (IPCC, Parry, 2007) with a concomitant rise of more than 1°C in sea surface temperature since the 1950s (Meredith & King, 2005). Significant research to date has focused on determining the effects of rising temperature on the magnitude of the spring bloom (Montes-Hugo *et al.*, 2009), but there is limited understanding of the mechanisms that control the rates of carbon fixation and consumption in these waters.

Photochemical reactions are nearly temperature independent and phytoplankton have developed several adaptive mechanisms to mitigate the effect of low temperature on the photosynthetic electron transport chain (see reviews by Mock & Hoch, 2005; Morgan-Kiss *et al.*, 2006; Dolhi *et al.*, 2013). As a result, the light reaction of photosynthesis is little affected by low temperature under nutrient-replete conditions. For the dark reaction, the reduced catalytic rates of various enzymes in the Calvin cycle at cold temperature can be partially compensated by the increased solubility of CO_2 over O_2 in water, an efficient carbon concentrating mechanism (Kranz *et al.*, 2014), and an increase in the cellular concentration of key enzymes, including Ribulose-1,5-bisphosphate carboxylase oxygenase, Rubisco (Young *et al.*, 2014). By contrast, respiratory processes have been reported to be highly sensitive to the change in temperature. Large decreases in respiration rate with decreasing temperature have been shown in previous studies of individual phytoplankton and macro-algae (Staehr & Birkeland, 2006; Padilla-Gamino & Carpenter, 2007), as well as in numerous ecosystems (Valentini *et al.*, 2000; Regaudie-de-Gioux & Duarte, 2012; Yvon-Durocher *et al.*, 2012). It is unclear why phytoplankton growing at a given growth rate would need less energy from respiration at low than at higher temperatures. One possibility is that psychrophilic phytoplankton may take advantage of the maintenance of the high activity of their photosystems to generate ATP via the photosynthetic apparatus.

In this study we used three different techniques to study primary production and respiration in the WAP (LTER-station B, Palmer station, Latitude: −64.7795; Longitude: −64.0725, sampling depth: 10 m, total depth *c.* 70 m; Supporting

Information Fig. S1) during the austral summer of 2012/2013. Comparing the results of three techniques provides insights into some of the mechanisms that control the primary productivity in the WAP. Two of these techniques are bottle incubations that measure production from the light reaction of photosynthesis ($H_2{}^{18}O$ incubation) or the dark reaction of photosynthesis ($^{14}CO_2$ incubation). In addition, measurements of biologically derived O_2 supersaturation, as well as of the isotopic composition of the O_2 pool, from *in situ* sample collection, allowed us to derive time-integrated ratios of Net/Gross production (the 'triple oxygen isotope technique'; Luz & Barkan, 2000; Prokopenko *et al.*, 2011; Juranek & Quay, 2013). To further explore the underlying physiological processes, laboratory experiments were conducted with the model psychrophilic diatom *Fragilariopsis cylindrus*, including measurements of net and gross photosynthesis, respiration and cyclic electron flow.

Materials and Methods

Field sampling and incubation experiments

Sampling took place twice weekly in the morning at LTER-station B (Latitude: −64.7795; Longitude: −64.0725; total depth *c.* 70 m). Water from 10-m depth was collected (monsoon pump; Waterra WSP-SS-80-NC) and dispensed into acid washed (10% HCl) containers, rinsed thoroughly with MilliQ and on-site water, for transport back to the shore-based laboratories. Back at shore, all containers were kept in a cold room (2°C) until processing, which typically occurred within 1–2 h of sample collection. Incubation experiments (described below) were conducted on sub-samples placed in a flow-through seawater tank shaded with neutral density screening to reduce irradiance by 50% (*LEE* filters 209 0.3ND). A continuous flow of seawater pumped from the shore (10-m depth) was used for temperature control.

Pigment measurements and identification

A known volume of sample (0.2–1 l) was collected in duplicate and filtered onto a glass fiber filter (Whatman GF/F, nominal pore size = 0.7 μm). After overnight extraction in 90% acetone at −20°C, chlorophyll *a* (Chl*a*) concentration for each duplicate was determined with a fluorometer (Turner Designs 10-AU), measuring the un-acidified and acidified sample to correct for phaeopigments (Welschmeyer, 1994). For pigment identification (chlorophyll and carotenoids), one liter of seawater was filtered under low light onto a GF/F, wrapped in aluminum foil, flash frozen in liquid nitrogen and subsequently stored at −80°C. Phytoplankton species composition for the three major taxa (diatoms, *Phaeocystis* and cryptophytes) was determined from the abundance of the pigments fucoxanthin, 19′ hexanoyloxyfucoxanthin and alloxanthin (Everitt *et al.*, 1990; Arrigo *et al.*, 2000). Quantification of pigments was conducted using HPLC analysis at the Estuarine Ecology Lab (University of South Carolina) following the protocol described in Pinckney *et al.* (1998).

Seawater hydrography and meteorological measurements

The Palmer station Long Term Ecological Research (PAL-LTER) program conducted regular depth profiles of temperature and salinity at LTER-station B using a Seabird SBE 19plus Seacat Profiler. These depth profile (Fig. S2) measurements were made within 1–2 h of our regular sampling times. Seawater density (Fig. S3) was computed from salinity and temperature using the TEOS-10 seawater equation of state (http://www.teos-10.org/software.htm). Surface PAR intensities (i.e. irradiance between 400 and 700 nm wavelength) were measured by the Palmer Station Terra Laboratory using a Li-Cor LI-190SA quantum sensor. Wind-speed data were obtained from the meteorological sensors on top of the Palmer Station Terra Laboratory.

O_2 measurements

Dissolved [O_2] was measured by Winkler titration. Seawater was collected with a Go-flo bottle and transferred directly to Winkler bottles, taking care to avoid bubbles and to seal samples and reagents with no headspace. Samples for each sampling day were taken in duplicate. Titrations were performed using an amperometric oxygen titrator designed by Dr Chris Langdon (Langdon, 1984; Culberson & Huang, 1987).The instrumental precision of the measurements is ± 2 μmol l^{-1} but the average precision of the duplicate was ± 4 μmol l^{-1}.

$H^{18}O_2$ incubations

Gas-tight bottles (145 ml, Pyrex) were rinsed and filled with collected seawater from the carboys. One bottle was set aside for immediate transfer (initial sample), whereas two bottles were spiked with 125 μl $H_2{}^{18}O$ (Medical Isotopes, 97.6%) for a final enrichment of 412.4‰. The two experimental bottles were incubated for 4–8 h in the aquarium tank outside the station. For our laboratory experiments we followed the same procedure except that duplicate bottles were taken for immediate transfer (initial samples) and duplicate bottles were incubated in an illuminated incubator (150 μmol m^{-2} s^{-1}) at 0.5°C. The samples were subsequently transferred into custom-made 500-ml flasks equipped with Louwers-Hapert valves (LH flask), that had been previously spiked with 100 μl of saturated $HgCl_2$, dried and evacuated (*c.* 1.5 mTorr = *c.* 0.2 Pa). The LH flasks were then analyzed back in the laboratory at Princeton within 6 months. Before analysis, the liquid phase was first equilibrated, and then carefully drained. LH flasks were then put in a freezing bath and the gas in each flask transferred into a stainless steel tube kept in a liquid helium tank. Each tube was allowed to warm up for 1 h before analysis in a Delta Plus XP mass spectrometer for dO_2/Ar, $d^{18}O$ and $d^{15}N$ (see Emerson *et al.*, 1995). The increase of [$^{18}O^{16}O$] provides a measurement of Gross photosynthesis (GP) in the bottle, whereas the change in [O_2] during the incubation provides the net production in the light in the bottle (NBP_L). The difference of the two gives respiration in the light in the bottle. The errors were calculated as standard deviation of the duplicates. The values were converted from oxygen evolution to carbon fixation

using a photosynthetic quotient (*PQ*) based on C : N ratios from Young *et al.* (2014) and derived from electrons balance:

$$PQ = \frac{\text{mol } O_2}{\text{mol C}} = \frac{\frac{1}{4}\text{mol } e^-}{\text{mol C}} = 1 + 2 * \frac{N}{C}.$$

This equation assumes that all nitrogen source is NO_3^- and an average photosynthetic product of $CH_{2+3N/C}\,ON_{N/C}$.

All the measurements and values used can be found in Table S1.

^{14}C incubations

We used a ^{14}C-based incubation approach to measure C fixation rates by phytoplankton assemblages. Samples were incubated in polycarbonate bottles (125 ml), with varying amounts for $NaH^{14}CO_3$ in the flow-through seawater tank. Triplicate samples for Gross Primary Production (GPP) measurements were spiked with 10 μCi $H^{14}CO_3^-$ and incubated in the tank for 2 h. Both incubations were initiated at midday. Triplicate samples for Net Primary Production (NPP) were spiked with 5 μCi $H^{14}CO_3^-$ and incubated for 24 h. In addition to the six NPP and GPP bottles, two bottles were used as controls and spiked with 5 μCi $H^{14}CO_3^-$; one bottle was filtered immediately after addition (blank), whereas the other was incubated in the dark for 24 h in the seawater tank (negative control).To quantify total ^{14}C activity for specific activity calculations, a subsample (125 μl) was collected from each bottle after the incubation period. Subsequently, samples were filtered onto a 0.7-μm glass fiber filter, which was placed into 20-ml scintillation vials and acidified with 6 N HCl for at least 24 h. Radioactivity in the samples was measured by scintillation counting on a Beckman-Coulter Liquid Scintillation counter (LSC 6500), using a standard quench curve correction to derive disintegrations per minute. The errors were calculated as standard deviation of the triplicate. An estimation of the correction for respiration of unlabeled carbon during the 24-h experiment was also calculated (see Notes S1).

In situ measurement of $\Delta O_2/Ar$ and triple oxygen isotopes

Samples were collected with a Go-flo bottle and transferred immediately into 500-ml custom-made pre-evacuated and pre-poisoned bottles with Louwers-Hapert (LH) valves (Emerson *et al.*, 1995). Great care was taken during the sample collection process to avoid entrainment of atmospheric oxygen. The samples were stored at ambient temperature and analyzed at Woods Hole Oceanographic Institution within 6 months. Analysis followed the method of Barkan & Luz (2003) with the modification that the GC column was 5.3 m and held at −3°C, and that each sample was collected on a cryogenic trap at < 10°K which was then warmed to room temperature and directly released into an isotope ratio mass spectrometer. The ratio O_2/Ar reflects the mass balance between NCP and gas exchange (Craig & Hayward, 1987; Emerson *et al.*, 1991), whereas the triple oxygen isotope measurement reflects the mass balance between GPP and gas exchange (using the equation described in Prokopenko *et al.*, 2011). The details of this approach have been described previously (Luz & Barkan, 2000; Reuer *et al.*, 2007) and are explained in Notes S2. Values for NCP and GPP were converted from μmol $O_2\,m^{-2}\,d^{-1}$ to μmol $O_2\,l^{-1}\,d^{-1}$ using the computed mixed layer depth (derived from a density difference criterion of 0.125 $kg\,m^{-3}$) or our sampling depth of 10 m, whichever was greater.

Bacterial productivity and respiration

Thirty millilitre bottles were filled with seawater sub-samples. Triplicate control bottles were immediately spiked with 200 μl formalin (37% formaldehyde) to stop biological activity. All bottles were then spiked with 50 μl ^3H-thymidine. The biologically active bottles (in triplicate) were then incubated in the outdoor seawater tank for 2 h. At the end of the incubation, biological activity was stopped by adding 200 μl formalin. A subsample was taken from all bottles for specific activity determination, whereas the remaining volume was filtered on a 0.2-μm cellulose nitrate filter. The filters were dried overnight, dissolved in ethyl acetate, and counted on a Beckman–Coulter Liquid Scintillation counter (LSC 6500), with quench correction. Following (Kirchman *et al.*, 1982), the uptake rate of labelled compound $v(t)$ is assumed to be proportional to the bacterial growth rate: $v(t) = \frac{1}{C} \times \frac{dN(t)}{dt}$ (N, number of cells; conversion factor $C = 1.2 \times 10^6$ cells $pmol^{-1}$ (Delille & Cahet, 1997)). Bacterial production and respiration were calculated using an average value of 10 fgC per cell and a growth efficiency factor of 0.15 (Ducklow *et al.*, 2012). Errors were calculated as standard deviation of the triplicates.

Laboratory culture experiments

Fragilariopsis cylindrus (CCMP 1102) was grown in semi continuous batch culture using 0.2-μm-filtered coastal seawater supplemented with Aquil nutrients (Sunda *et al.*, 2005) under continuous light (*c.* 150 μmol $m^{-2}\,s^{-1}$) at 0.5°C. Cell densities were counted with a Coulter Counter Z2 (Beckman Coulter Inc., Fullerton, CA, USA). Cells were harvested during the exponential phase after *c.* 2 wk of growth. Incubations with $H_2{}^{18}O$ in the light were performed (as described above) to yield estimates of net and gross photosynthesis as well as respiration in the light. Additional incubations were performed in the dark to derive estimates of respiration in the dark from the change in O_2 concentration.

Cyclic electron flow

For the determination of relative cyclic electron transport rates, *F. cylindrus* cells in exponential growth were filtered gently and resuspended into Aquil medium with 20% w/w Ficoll. Following continuous illumination during which the redox state of P_{700} in PSI reaches steady-state, the reduction rate of P_{700} was measured in the dark by fast spectrophotometry as the increase in absorbance at 700 nm (JTS-10 spectrophotometer; BioLogic, Claix, France). The total number of PSI as well as the rate of their dark

reduction, due to either cyclic or linear electron flow, was obtained by the technique reviewed in Alric (2010). To discriminate between the cyclic and linear electron flow, the measurements were done under two different conditions: without any inhibitor and in the presence of DCMU (3-(3,4-dichlorophenyl)-1,1-dimethylurea, 20 μM), a specific inhibitor of PSII that blocks the linear flow of electrons going to PSI. To obtain the initial rate of P_{700} reduction, the spectroscopic data were fitted with an exponential function and corrected for an instrumental artefact as explained in supplemental information (Notes S3).

Results

Community composition and phytoplankton biomass

The near-shore waters adjacent to Palmer station are typically ice-covered in the winter. During the austral spring 2012, the ice retreated at the end of October (*c.* 25 October). A large bloom of phytoplankton was observed in late November–early December of 2012 (up to 45 μg Chl*a* l^{-1}; Fig. 1a). Based on the analyses of three marker pigments (fucoxanthin, 19′-hexanoyloxyfucoxanthin and alloxanthin, see Arrigo *et al.*, 2000), the phytoplankton community at the beginning of the season was equally dominated by diatoms and *Phaeocystis* (Fig. 1a). As the diatom bloom developed, the *Phaeocystis* share of the community decreased and at the peak of the bloom the population was essentially all diatoms. The bloom was interrupted by a mixing event which temporarily reduced the chlorophyll concentration down to 10 μg l^{-1} (on 4 December). In mid-December, the bloom crashed and thereafter the phytoplankton population, then dominated by cryptophytes and *Phaeocystis*, was maintained *c.* 1–3 μg Chl*a* l^{-1}. The abundance of macronutrients at the crash of the bloom and during the rest of the season (Fig. S4) suggests that the end of the bloom and thereafter control of the population was likely due to grazing (Tortell *et al.*, 2014). In early March, a smaller bloom of diatoms and *Phaeocystis* yielded a chlorophyll concentration slightly above 6 μg l^{-1}.

Photosynthesis and respiration during daylight

In order to study photosynthesis and respiration in the light, incubations with $H_2{}^{18}O$ were performed weekly on water collected from LTER-station B, starting at midday and lasting 4–8 h. The rates of both net and gross production in the bottle are given in units of μmol l^{-1} d^{-1} but only pertain to the period of the incubation. These incubations thus included the daily irradiance peak *c.* 15:00 h and were all done at saturating light. We observed no relationship between average PAR during the incubations and the Chl*a* –normalized photosynthetic rates (Fig. S5), suggesting that photoinhibition or light limitation were not occurring. Net bottle production in the light (NBP_L), defined as the difference between photosynthetically produced oxygen and respiratory O_2 consumption by the autotrophs and heterotrophs in the bottle, was measured by ΔO_2, the difference between the final and the initial O_2 concentration in the incubation bottle. Early in the season (before 14 November), the incubations showed a net heterotrophy during daylight as shown by a slightly negative NBP_L (Fig. 1b). This net heterotrophy was confirmed by *in situ* measurement of dO_2/Ar with a Membrane Inlet Mass

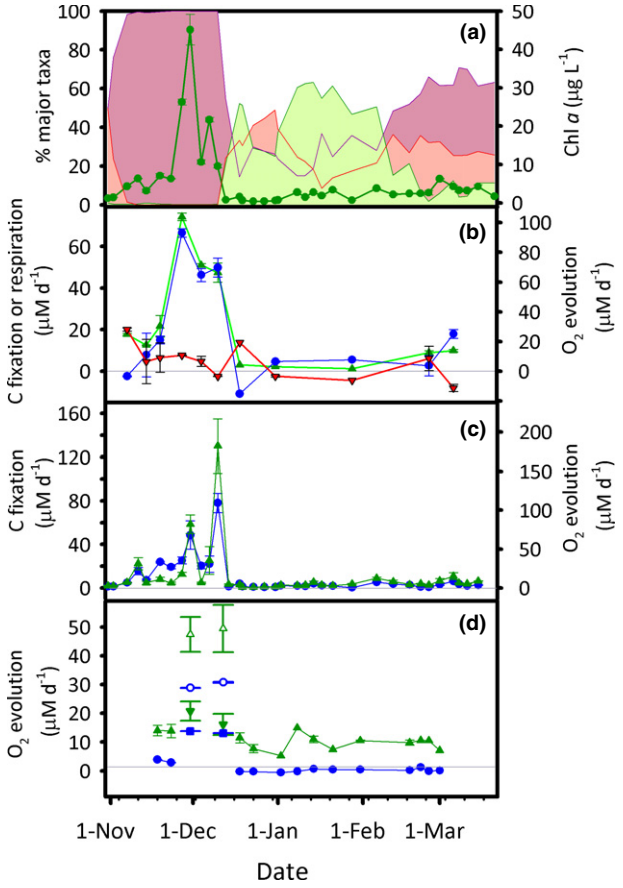

Fig. 1 (a) Chl*a* and community composition for three taxa during the austral spring and summer at Palmer Station. Diatoms are represented by the purple area, *Phaeocystis* by the orange area, cryptophytes by the green area. All areas are extrapolated from discrete measurements. Chl*a* is represented by the dark green curve. Error bars represent standard deviation of duplicates. (b) Results from day-time incubations with $H_2{}^{18}O$. Blue circles, net bottle production in the light (NBP_L) defined as $([O_2]_{final}-[O_2]_{initial})$; green triangles, Gross Photosynthesis (GP) defined as the production rate of $[^{18}O^{16}O]$; red triangles, respiration in the light (R_L) defined as $R_L = GP–NBP_L$. Error bars represent standard deviation of duplicates. All rates are normalized for 1 d but only pertain to the period of incubation. The left and right axes are stoichiometrically equivalent with a photosynthetic quotient PQ = 1.4 (c) Results from incubations with ^{14}C. Blue circles, net primary production (NPP), measured from 24 h incubations. Green triangles, Gross Primary Production (GPP), measured from 2 h incubations. GPP rates are normalized for 1 d but only pertain to the period of incubation. The values have been converted from carbon fixation to oxygen evolution using a PQ = 1.4. Error bars represent standard deviation of triplicates. (d) Results from the *in situ* measurements. Blue, Net Community Production (NCP), derived from dO_2/Ar. Green, Gross Primary Production (GPP), derived from triple oxygen isotope. Closed triangles and closed circles have been calculated assuming steady-state conditions and that samples were within the mixed layer. For the two peaks of the bloom: open triangles and open circles assume nonsteady-state and samples within the mixed layer. Closed downward triangles and squares assume nonsteady-state and samples below the mixed layer. No point is shown for 5 December as we could not account for the vertical mixing on that date. Error bars represent standard deviation of duplicates.

Spectrometer (Tortell *et al.*, 2014). During the bloom (defined here as the period between 19 November and 10 December 2012 when the chlorophyll was above 5 μg Chl*a* l^{-1}), we measured a very high NBP_L with a maximum > 90 μmol O_2 l^{-1} d^{-1} corresponding to > 65 μmol C l^{-1} d^{-1} (using an average photosynthetic quotient PQ = 1.39; Fig. 1b). For the rest of the season, NBP_L values less than 6 μmol C l^{-1} d^{-1} were obtained until the second bloom, when values increase to *c.* 18 μmol C l^{-1} d^{-1}.

In the same bottles, Gross Photosynthesis (GP; defined as the amount of oxygen produced from the splitting of water during photosynthesis) was also measured, independently of NBP_L, as the increased concentration of $^{18}O^{16}O$ in incubations with $H_2{}^{18}O$ (see the Materials and Methods section). During most of the season the measured ^{18}O-derived GP closely tracked the measured ΔO_2-derived NBP_L (Fig. 2a). The correlation between the two (0.89 ± 0.08; $R^2 = 0.89$) in these incubations is dominated by the high values during the bloom and indicates that during several hours at midday net production in the bottle was *c.* 90% of GP. Thus, respiration at midday during the bloom, calculated as the difference of GP minus NBP_L during the incubation, was only *c.* 10% of GP. This respiration includes respiration by autotrophs (mitochondrial respiration and photorespiration), respiration by heterotrophs (mainly bacteria, as larger heterotrophs are excluded from the incubation bottles) and potentially the reduction of O_2 in the Mehler reaction. Bacterial respiration, derived from thymidine incorporation measured in separate 2 h incubations at midday, was less than 2 μmol C l^{-1} d^{-1} during the season at 10 m depth, except at the crash of the bloom when it increased to *c.* 8 μmol C l^{-1} d^{-1} (14 December, see Notes S4 and Fig. S6). After the crash of the first bloom, our ΔO_2 measurements in the incubations revealed very low overall net production (see Table S1).

Gross photosynthesis in the ^{18}O bottle incubations varied linearly with chlorophyll (Fig. 3) up to *c.* 25 μg l^{-1}. The slope of 3.0 μmol C μg^{-1} Chl*a* d^{-1} is similar to the values from the Antarctic reported by Westwood *et al.* (2010) (4.1 ± 1.7 μmol C μg^{-1} Chl*a* d^{-1} between 0 and 25 m) and by DiTullio *et al.* (2003) (5.6 ± 4.6 μmol C μg^{-1} Chl*a* d^{-1} in the Antarctic zone). The linearity of Fig. 3, despite the variability of the light intensity among experiments (PAR *c.* 200 to *c.* 670 μmol m^{-2} s^{-1}), indicates that photosynthesis was likely light-saturated during those incubations (see Fig. S5).

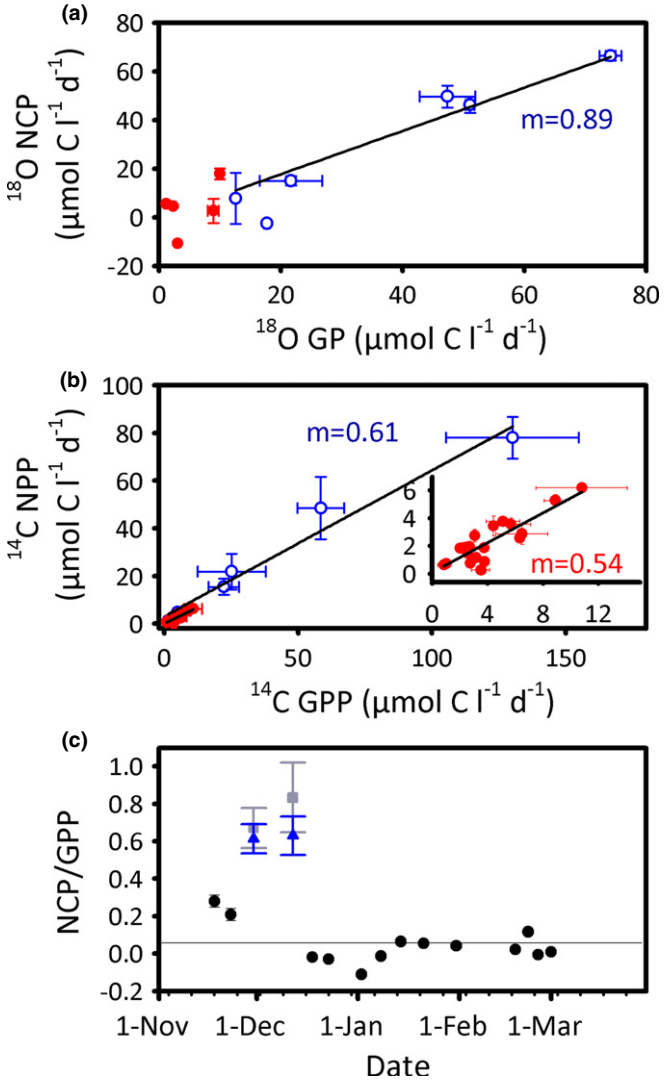

Fig. 2 Relation between Gross Primary Production (GPP) and Net Community Production (NCP) studied with three different techniques. Open circles, values before and during the bloom; red closed circles, values after the bloom; black closed circles, are NCP/GPP ratios. In each case *m* indicates the slope of the linear regression for each set of data. (a) Incubations in the light only – $\Delta O_2/^{18}O$ method. The values have been converted from oxygen evolution to carbon fixation using a photosynthetic quotient PQ = 1.4. Error bars represent standard deviation of duplicates. (b) Incubations during a light-dark cycle – ^{14}C method (24 h and 2 h incubations). The inset is a blow-up of the data obtained after the bloom. Error bars represent standard deviation of triplicates. (c) Ratio of NCP/GPP from *in situ* measurements (dO_2/Ar and $^{17}\Delta$). Black circles assume steady-state and samples within the mixed layer. Gray squares assume nonsteady-state and samples below the mixed layer. Blue triangles assume nonsteady-state and samples above the mixed layer. Error bars represent standard deviation of duplicates.

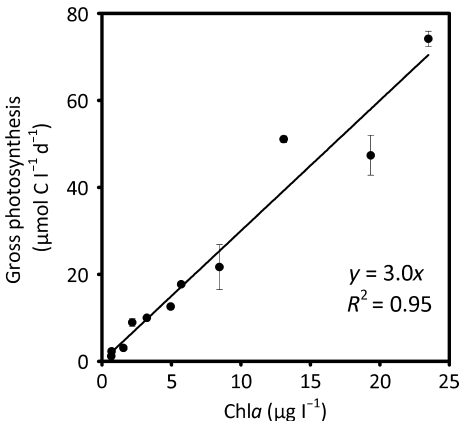

Fig. 3 Correlation of ^{18}O derived-Gross photosynthesis (converted in carbon unit using PQ values obtained for each samples as explained in the Materials and Methods section) and Chl*a*. Error bars represent standard deviation of duplicates.

Photosynthesis and respiration during a light–dark cycle using ^{14}C

In order to measure net and gross primary production during a full diel cycle, 2 and 24 h $^{14}CO_2$ uptake incubations were performed twice weekly starting around midday. Net Primary Production (NPP) measured in 24-h experiments represents the gross carbon fixation minus DOC excretion and respiration by the autotrophs and heterotrophs present in the incubation bottles (excluding large zooplankton). A somewhat lower value for a net primary production NPP*, is obtained by subtracting from the measured NPP an estimate of the unlabeled carbon respired during the 24-h incubation (see Notes S1). Due to a mixing event (that was not captured by an ^{18}O incubation) those incubations showed two peaks of high net production during the bloom (Fig. 1c), reaching up to 78 μmol C l^{-1} d^{-1} on 10 December. Differences in the relative values of net production measured by ^{14}C and ^{18}O incubations result, in part, from differences in the duration of light saturation during the two types of experiments. During the rest of the season the ^{14}C based NPP values were generally < 2 μmol C l^{-1} d^{-1}.

The average ratio of ^{14}C-NPP/^{18}O- NBP = *c.* 0.79 during the bloom and 0.20 after the crash of the bloom, illustrates the fact that the two methods measure different processes (see rest of the section). The average ratio ^{18}O-GP/^{14}C NPP = *c.* 3.57 measured for the entire season up to the second bloom is similar to previously reported values in the laboratory (Halsey *et al.*, 2013) and is within the range of the values reported from the field (Bender *et al.*, 1999; Laws *et al.*, 2000; Marra, 2007; Hamme *et al.*, 2012).

Gross primary production (GPP), which represents the CO_2 fixed by the autotrophs into new biomass, was measured in separate bottles spiked with $^{14}CO_2$ and incubated at the same time and in the same tank as NPP but for only 2 h at midday. The rates are given in μmol l^{-1} d^{-1} but only pertain to the 2 h period of incubation. Surprisingly, some of the measurements at the beginning of the season and during the bloom gave GPP values that were lower than the NPP. Such ratios of ^{14}C-NPP/^{14}C-GPP > 1 have been observed previously (Robinson *et al.*, 2009) and may reflect a reduced photosynthetic activity at midday.

Omitting the data where ^{14}C GPP was lower than NPP, we observe a strong correlation between NPP and GPP (Fig. 2b) with a slope of 0.61 ± 0.05 before/during the bloom and a slope of 0.54 ± 0.07 afterward. Those slopes are somewhat lower when respiration of unlabeled carbon is taken into account (NPP* vs GPP: 0.54 before/during the bloom and 0.24 after the bloom). Those ratios of net production to gross photosynthesis are much lower than our value of *c.* 0.9 from the ^{18}O incubations obtained at midday. Part of the explanation is the difference in timing between the ^{18}O and ^{14}C incubations, with only the latter measurements including the dark portion of the day. Differences in the diel patterns of photosynthesis and respiration rates (Moline & Prezelin, 1996) would also lead to discrepancies between the two methods, as would excretion of some of the organic carbon (which is accounted for in the ^{18}O but not in the ^{14}C experiments).

Photosynthesis and respiration: time- integrated *in situ* measurements

The triple oxygen isotope method provides an *in situ* measure of time-integrated gross and net production of the whole community, without any exclusion or constraints linked to bottle incubations (Luz & Barkan, 2000). Net community production in this case is derived from the supersaturation of O_2 compared to Ar which represents the balance of photosynthesis, respiration and gas exchange (computed using a wind-speed-dependent parameterization of mixed layer gas exchange coefficients, according to Wanninkhof (1992)). Gross photosynthesis in the mixed layer is calculated from the isotopic composition of the O_2 pool, which is determined by the gross O_2 fluxes associated with photosynthesis (splitting of water) and air–sea exchange. The calculations of NCP and GPP were made considering that the samples were within the mixed layer and that oxygen was at steady-state, except during the peak of the bloom when the changing isotopic ratios were taken into account in order to calculate rates without necessitating the steady-state assumption (Kaiser, 2011; Prokopenko *et al.*, 2011). In addition, the calculations of NCP and GPP during the bloom were made considering that the sampling depth of 10 m was either below the mixed layer (as indicated by the density profiles; Fig. S2) or possibly within it (as indicated by the Ekman depth; Brody & Lozier, 2014). Details of the calculations to obtain NCP, GPP and their ratios, using different hypotheses of steady-state and mixed-layer conditions, can be found in aqTables S2 and S3, and Notes S2. No matter what the method (i.e. steady-state or time-varying, within mixed layer or below it), the rates of GPP and NCP during the bloom period are much higher than the rates of GPP and NCP during the rest of the season.

Qualitatively, the triple oxygen isotope-derived NCP and GPP estimates (Fig. 1d) resemble those from ^{14}C incubations exhibiting two peaks during the bloom and remaining low afterward (except for an unexplained peak in GPP on 8 January). The absolute values in Fig. 1(d), however, are lower than in Fig. 1(b,c). This is in part due to the inherent time and space averaging of the triple oxygen isotope method, which necessarily smoothes out the high values. This integrated measure of NCP demonstrates that the system never reached a sustained period of net heterotrophy before or after the bloom with only a few values of NCP slightly below zero.

The NCP/GPP ratio measured with the dO_2/Ar and triple oxygen isotope technique started with values *c.* 0.25 at the beginning of spring and increased to values above 0.6 during the two peaks of the bloom (regardless of the assumption made regarding the depth of the mixed layer). These high ratios observed in both NCP/GPP from *in situ* measurements and NPP/GPP from ^{14}C data, indicated that community respiration was largely controlled by the microorganisms that were sampled in the bottles, as opposed to large grazers that would have been excluded. Thymidine incorporation measurements indicate very low bacterial production and respiration before and during the bloom (Fig. S6), implying that much of the respiration was attributable to the phytoplankton. Just at the crash of the bloom the O_2 NCP/GPP decreased to low and possibly negative values as expected and

confirmed by estimates of high bacterial respiration based on thymidine incorporation data (Fig. S6). During the rest of the season we observed a low positive NCP/GPP ratio ranging between *c.* −0.1 and *c.* 0.1, much lower than the ratio of 0.54 obtained from the ^{14}C data. This large difference likely reflects the activity of large grazers which are excluded from the ^{14}C incubation bottles but keep the algal population and the net community production low (Tortell *et al.*, 2014). Our observations thus suggest that autotrophic respiration dominated community O_2 consumption during the pre-bloom and bloom phases of the seasonal cycle, whereas large grazers (e.g. krill) accounted for most of the community respiration during the later months.

Physiological data from the polar diatom *Fragilariopsis cylindrus*

Because diatoms were the major taxa during the bloom, we conducted experiments with the psychrophilic organism *F. cylindrus* in laboratory cultures maintained at 0.5°C under continuous light. $H_2{}^{18}O$ incubations (*c.* 9 h) on those light-adapted cells gave values of 0.38 and 0.12 pmol O_2 per cell d^{-1} for gross photosynthesis and respiration in the light, respectively, whereas incubations in the dark gave a value of 0.07 pmol O_2 per cell d^{-1} for respiration in the dark (Fig. 4a). Based on these data, we calculated a ratio for the daily integrated net and gross production for a diel cycle with 20 h : 4 h, light : dark (similar to the diel cycle during the bloom) of NP_D/GP of 0.65. This value represents an average value for the light period because our cultures were grown under continuous light and thus were not synchronized to a diel cycle like the community in the WAP. Nonetheless, this value is very close to the those we obtained in the field during the bloom from *in situ* measurements (Fig. 2c). To the extent that the ratio obtained with *F. cylindrus* can be extrapolated to the diatoms in the WAP, these results provide further evidence that the community respiration measured during the bloom was dominated by the phytoplankton. This is consistent with our estimations of low heterotrophic respiration in the field based on thymidine incorporation rates (see Notes S4) and with previous studies (Ducklow *et al.*, 2012).

It has been suggested that cyclic electron flow (CEF) generates substantial ATP in psychrophilic green algae from Antarctic lakes (Morgan-Kiss *et al.*, 2002; Dolhi *et al.*, 2013). Such a mechanism could help explain the very low respiration rates we observed at midday in the field (with the $H_2{}^{18}O$ incubations) as well as the previously reported high concentration of ATP in psychrophilic organisms (Napolitano & Shain, 2005). In CEF, light absorption and charge separation in PSI is followed by an electron transfer back to the b6f complex, via a ferredoxin, and the beginning of a cycle through the plastoquinone pool (Falkowski & Raven, 2007). Each cycle transports protons from the stroma to the lumen, generating a proton gradient, which leads to the production of ATP via the ATP synthase in the thylakoid membrane (see Eberhard *et al.*, 2008 for review). Re-reduction of PSI can occur through the linear flow of electron from PSII or from CEF. Using laboratory cultures of *F. cylindrus*, we obtained the first estimates of the relative importance of CEF and linear electron

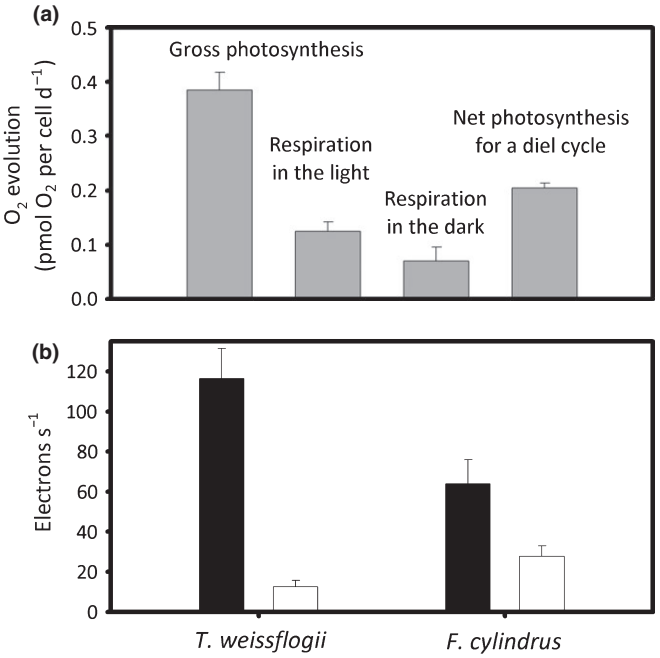

Fig. 4 (a) Gross photosynthesis and respirations of *Fragilariopsis cylindrus*. Incubation with $H_2{}^{18}O$ gives gross photosynthesis and respiration in the light (mitochondrial respiration in the light + photorespiration). Incubation in the dark gives mitochondrial respiration in the dark. From those results we calculated a net photosynthesis over a light : dark diel cycle of 20 h : 4 h. Error bars represent standard deviation of duplicates. (b) Relative electron flow through PSI in the presence (open bars) and absence (closed bars) of DCMU – comparison of *F. cylindrus* and *Thalassiosira weissflogii*. The maintenance of a high electron flow in the presence of DCMU in *F. cylindrus* is indicative of an active cyclic electron flow. Error bars represent standard deviation of duplicates.

flow in a psychrophilic diatom. The reduction rates of the PSI pool in the presence and absence of DCMU (an inhibitor of linear electron flow) were compared using a fast spectrophotometric method (see Alric, 2010 for review). The maintenance of a rapid reduction rate of PSI (*c.* 30 $e^- s^{-1}$) in *F. cylindrus* (at 0°C) in the presence of DCMU (Fig. 4b) is indicative of an active CEF. By contrast, for *T. weissflogii* at 25°C the electron flow decreased to low values in the presence of DCMU (< 15 $e^- s^{-1}$; Fig. 4b), indicating minimal CEF in this species under these conditions. Such a low rate of PSI reduction in the presence of DCMU in *T. weissflogii* could also result from the breakdown of starch to produce NADPH (Alric *et al.*, 2010).

Discussion

We used three different techniques to measure primary production during our field season: two *in vitro* techniques (^{18}O incubations, ^{14}C incubations) and one *in situ* method (dO_2/Ar and triple oxygen isotopes). These techniques measure different parameters over different time periods and provide complementary insights into the processes responsible for the metabolic balance of the planktonic ecosystem. Notably, all three methods demonstrated a high amount of net production during the diatom spring bloom, which, although not atypical, appears to have been one of the largest on record during the 25 yr of observation

at the Palmer Station LTER site (http://oceaninformatics.ucsd.edu/datazoo/data/pallter/datasets). According to the LTER data archive, there were 15 yr between 1991 and 2011 when the chlorophyll concentrations exceeded 10 $\mu g\,l^{-1}$, and 8 yr when they exceeded 30 $\mu g\,l^{-1}$. During our field season, the chlorophyll concentration reached 45 $\mu g\,l^{-1}$, concomitant with a gross production rate of 75 $\mu mol\,C\,l^{-1}\,d^{-1}$ (Fig. 1b). Using the relationship derived between ^{18}O-GP and chlorophyll (Fig. 3), we estimate that the bloom accounted for nearly 60% of the gross production during the entire summer season. This particular bloom provided an opportunity to better understand the processes that allow high primary productivity in very cold waters. Our data indicate that heterotrophic processes played a minimal role during the spring bloom and that all metabolic processes were dominated by autotrophs. This explains why both ^{14}C and the *in situ* (dO_2/Ar and $^{17}\Delta$) measurements, gave similarly high ratios of net/gross production, with maximum values greater than 0.54. For comparison, most published ratios of net-to-gross production based on dO_2/Ar and $^{17}\Delta$ data in low temperature seawater are below 0.2 (Castro-Morales *et al.*, 2013), (Juranek *et al.*, 2012), with a few values above: 0.35 on average during spring bloom conditions in the subpolar North Atlantic Ocean (Quay *et al.*, 2012), up to 0.43 in the WAP (Huang *et al.*, 2012), and *c.* 0.50 in the Bering Sea (Prokopenko *et al.*, 2011).

Taken at face value, the results of our ^{18}O incubations during the bloom indicate that most of the electrons obtained from the splitting of water result in net carbon fixation during midday. This means that photorespiration and mitochondrial respiration, as well as the Mehler reaction, were kept to a minimum in the diatoms at Palmer station at midday. The extent of photorespiration depends on the relative affinity of Rubisco for CO_2 and O_2 which are competing for binding at the active site. As in higher plants, the O_2 turnover rate in the Rubisco of diatoms is slower than that of CO_2. The Rubisco of diatoms can also exhibit a half-saturation constant for oxygen up to eight times that of higher plants (Badger *et al.*, 1998). Further, it has been shown in plants (Tcherkez *et al.*, 2006) and in phytoplankton (Haslam *et al.*, 2005) that low temperature increases the specificity of Rubisco for CO_2 over O_2. Together with an efficient CCM in the cells (see Kranz *et al.*, 2014), the increased CO_2 specificity of Rubisco (Young *et al.*, 2014) should act to maintain low photorespiration relative to C fixation in psychrophilic diatoms.

Cyclic electron flow, CEF, allows cells to produce ATP directly from sunlight without evolving oxygen or fixing carbon, and independently of mitochondrial respiration. To the extent that this mechanism for ATP production depends principally on photochemical processes, it should be less sensitive to temperature than the multiple enzymatic reactions of the Krebs cycle. This requires that the activity of the enzymes involved in the CEF and ensuing ATP production, especially ATP synthase in the thylakoid membrane, be maintained at a high level either by adaptation to cold or by a higher protein concentration. A significant role for cyclic electron flow has been reported previously in an Antarctic green alga from Lake Bonney (Dolhi *et al.*, 2013). The Mehler reaction is in competition with the cyclic electron flow in PSI. Our ^{18}O incubation data during the bloom imply that, like photorespiration, mitochondrial respiration and the Mehler reaction are minimal at midday in Antarctic diatom; this may be associated with an intense CEF activity. Our laboratory experiment with *F. cylindrus* confirmed that this process is indeed physiologically important in this polar diatom. High intracellular ATP concentrations previously reported in two psychrophilic green algae (Napolitano & Shain, 2005) would also be consistent with a high CEF activity. Interestingly, in those psychrophilic species, ATP concentrations were reported to increase with decreasing temperature, whereas the opposite trend is observed in mesophilic and thermophilic organisms.

The very low respiration measured during our ^{18}O incubation during the bloom at midday (*c.* 10% of GP) is somewhat difficult to reconcile with the ^{14}C incubation and *in situ* measurements that show a net-to-gross ratio on the order of 0.6 (Fig. 2). If such a low respiration were maintained for the whole daylight period, it would mean that 30% of the photosynthate would have to be respired during the night to reconcile the numbers. This seems implausible considering that the night at Palmer lasted only 4 h during the height of the phytoplankton bloom. Alternatively, respiration by autotrophs (or heterotrophs) may also have been higher during early and late daylight hours than during midday. This would be consistent with a scenario in which the cells exploit the high photon flux at midday to generate ATP through cyclic electron flow. Conceivably, an intense CEF activity at the expense of linear electron flow during periods of high light could also explain low GPP measured in short term ^{14}C experiments. Clearly, additional information on the diel cycle of photosynthesis and CEF activity of psychrophilic diatoms should help us understand how the ratio of net/gross photosynthesis varies through the course of a day.

From an ecological perspective, an important implication of our data is the low ratio of community respiration/gross primary production during the diatom spring bloom at Palmer station. Based on our laboratory data with *F. cylindrus* we hypothesize that part of the reason why phytoplankton may be able to maintain relatively high productivity at low temperature even when their respiration rate falls (as it does at midday) is because they can generate ATP through cyclic electron flow. More generally the overall trend of decreasing R/P with decreasing temperature (Regaudie-de-Gioux & Duarte, 2012), that is a characteristic of ecosystems dominated by autotrophs, results not just from the temperature dependence of the rates of photochemical and biochemical reactions, but must also reflect particular adaptive strategies, such as CEF and the change in the concentration and substrate affinity of key enzymes such as Rubisco (Young *et al.*, 2014). A better understanding of these strategies would allow us to foresee the likely changes in the net productivity of marine ecosystems at high latitudes which are being subjected to rapid climate change.

Acknowledgements

We would like to acknowledge the exceptional assistance and support of the United States Antarctic Program support staff at Palmer station as well as the entire Palmer LTER science team. We are particularly thankful to Professor Hugh Ducklow for his

help with bacteria productivity measurements. We also thank Professor John Dacey for his assistance during sampling, Stefanie Strebel for her assistance at Palmer station, and Zoe Sandwith for her assistance in measuring triple oxygen isotopes. We are very grateful to Professor Paul Falkowski for letting us use his facilities and instrument to measure cyclic electron flow, and to Dr Benjamin Bailleul for his expert advice and patient help for cyclic electron flow measurements. We also wish to thank Professor Maria Prokopenko for her helpful comments. This study was supported by funds from the US National Science Foundation (Award numbers 1040965 and 1043593). Funding to P.D.T. was provided by the Natural Science and Engineering Research Council of Canada.

References

Alric J. 2010. Cyclic electron flow around photosystem I in unicellular green algae. *Photosynthesis research* **106**: 47–56.

Alric J, Lavergne J, Rappaport F. 2010. Redox and ATP control of photosynthetic cyclic electron flow in *Chlamydomonas reinhardtii* (I) aerobic conditions. *Biochimica et Biophysica Acta (BBA)-Bioenergetics* **1797**: 44–51.

Arrigo KR, DiTullio GR, Dunbar RB, Robinson DH, VanWoert M, Worthen DL, Lizotte MP. 2000. Phytoplankton taxonomic variability in nutrient utilization and primary production in the Ross Sea. *Journal of Geophysical Research: Oceans (1978–2012)* **105**: 8827–8846.

Arrigo KR, van Dijken GL, Bushinsky S. 2008b. Primary production in the Southern Ocean, 1997–2006. *Journal of Geophysical Research: Oceans (1978–2012)* **113**: C08004, doi: 10.1029/2007JC004551.

Arrigo KR, van Dijken G, Long M. 2008a. Coastal Southern Ocean: a strong anthropogenic CO_2 sink. *Geophysical Research Letters* **35**: L21602.

Badger MR, Andrews TJ, Whitney S, Ludwig M, Yellowlees DC, Leggat W, Price GD. 1998. The diversity and coevolution of Rubisco, plastids, pyrenoids, and chloroplast-based CO_2-concentrating mechanisms in algae. *Canadian Journal of Botany* **76**: 1052–1071.

Barkan E, Luz B. 2003. High-precision measurements of 17O/16O and 18O/16O of O2 and O2/Ar ratio in air. *Rapid communications in mass spectrometry* **17**: 2809–2814.

Bender M, Orchardo J, Dickson M-L, Barber R, Lindley S. 1999. In vitro O_2 fluxes compared with ^{14}C production and other rate terms during the JGOFS Equatorial Pacific experiment. *Deep Sea Research Part I: Oceanographic Research Papers* **46**: 637–654.

Brody SR, Lozier MS. 2014. Changes in dominant mixing length scales as a driver of subpolar phytoplankton bloom initiation in the North Atlantic. *Geophysical Research Letters* **41**: 3197–3203.

Castro-Morales K, Cassar N, Shoosmith DR, Kaiser J. 2013. Biological production in the Bellingshausen Sea from oxygen-to-argon ratios and oxygen triple isotopes. *Biogeosciences* **10**: 2273–2291.

Craig H, Hayward T. 1987. Oxygen supersaturation in the ocean: biological versus physical contributions. *Science* **235**: 199–202.

Culberson CH, Huang S. 1987. Automated amperometric oxygen titration. *Deep Sea Research Part A. Oceanographic Research Papers* **34**: 875–880.

Delille D, Cahet G. 1997. Determination of conversion factors for estimation of subantarctic marine bacterial production measured by H-thymidine Incorporation methodology. *Aquatic microbial ecology* **13**: 121–125.

DiTullio GR, Geesey ME, Jones DR, Daly KL, Campbell L, Smith WO. 2003. Phytoplankton assemblage structure and primary productivity along 170 degrees W in the South Pacific Ocean. *Marine Ecology Progress Series* **255**: 55–80.

Dolhi JM, Maxwell DP, Morgan-Kiss RM. 2013. Review: the Antarctic *Chlamydomonas raudensis*: an emerging model for cold adaptation of photosynthesis. *Extremophiles* **17**: 711–722.

Ducklow HW, Baker K, Martinson DG, Quetin LB, Ross RM, Smith RC, Stammerjohn SE, Vernet M, Fraser W. 2007. Marine pelagic ecosystems: the west Antarctic Peninsula. *Philosophical Transactions of the Royal Society B* **362**: 67–94.

Ducklow HW, Schofield O, Vernet M, Stammerjohn S, Erickson M. 2012. Multiscale control of bacterial production by phytoplankton dynamics and sea ice along the western Antarctic Peninsula: a regional and decadal investigation. *Journal of Marine Systems* **98**: 26–39.

Eberhard S, Finazzi G, Wollman F-A. 2008. The dynamics of photosynthesis. *Annual review of genetics* **42**: 463–515.

Emerson S, Quay P, Stump C, Wilbur D, Knox M. 1991. O_2, Ar, N_2, and 222Rn in surface waters of the subarctic ocean: net biological O2 production. *Global Biogeochemical Cycles* **5**: 49–69.

Emerson S, Quay P, Stump C, Wilbur D, Schudlich R. 1995. Chemical tracers of productivity and respiration in the subtropical Pacific Ocean. *Journal of Geophysical Research: Oceans (1978–2012)* **100**: 15873–15887.

Everitt D, Wright S, Volkman J, Thomas D, Lindstrom E. 1990. Phytoplankton community compositions in the western equatorial Pacific determined from chlorophyll and carotenoid pigment distributions. *Deep Sea Research Part A. Oceanographic Research Papers* **37**: 975–997.

Falkowski PG, Raven JA. 2007. *Aquatic photosynthesis*. Princeton, NJ, USA: University Press.

Halsey KH, O'Malley RT, Graff JR, Milligan AJ, Behrenfeld MJ. 2013. A common partitioning strategy for photosynthetic products in evolutionarily distinct phytoplankton species. *New Phytologist* **198**: 1030–1038.

Hamme RC, Cassar N, Lance VP, Vaillancourt RD, Bender ML, Strutton PG, Moore TS, DeGrandpre MD, Sabine CL, Ho DT. 2012. Dissolved O_2/Ar and other methods reveal rapid changes in productivity during a Lagrangian experiment in the Southern Ocean. *Journal of Geophysical Research: Oceans (1978–2012)* **117**: C00F12.

Haslam RP, Keys AJ, Andralojc PJ, Madgwick PJ, Inger A, Grimsrud A, Eilertsen HC, Parry MA. 2005. Specificity of diatom Rubisco. In: Omasa K, Nouchi I, De Kok LJ, eds. *Plant responses to air pollution and global change*. Tokyo, Japan: Springer, 157–164.

Huang K, Ducklow H, Vernet M, Cassar N, Bender ML. 2012. Export production and its regulating factors in the West Antarctica Peninsula region of the Southern Ocean. *Global Biogeochemical Cycles* **26**: GB2005, doi: 10.1029/2010GB004028.

Juranek L, Quay P. 2013. Using triple isotopes of dissolved oxygen to evaluate global marine productivity. *Annual Review of Marine Science* **5**: 503–524.

Juranek L, Quay P, Feely R, Lockwood D, Karl D, Church M. 2012. Biological production in the NE Pacific and its influence on air-sea CO_2 flux: evidence from dissolved oxygen isotopes and O_2/Ar. *Journal of Geophysical Research: Oceans (1978–2012)* **117**: C05022.

Kaiser J. 2011. Technical note: consistent calculation of aquatic gross production from oxygen triple isotope measurements. *Biogeosciences* **8**: 1793–1811.

Kirchman D, Ducklow H, Mitchell R. 1982. Estimates of bacterial growth from changes in uptake rates and biomass. *Applied and Environmental Microbiology* **44**: 1296–1307.

Kranz SA, Young JN, Hopkinson BM, Goldman JAL, Tortell PD, Morel FMM. 2014. Low temperature reduces the energetic requirement for the CO_2 concentrating mechanism in diatoms. *New Phytologist* **205**: 192–201.

Langdon C. 1984. Dissolved oxygen monitoring system using a pulsed electrode: design, performance, and evoluation. *Deep Sea Research Part A. Oceanographic Research Papers* **31**: 1357–1367.

Laws EA, Falkowski PG, Smith WO, Ducklow H, McCarthy JJ. 2000. Temperature effects on export production in the open ocean. *Global Biogeochemical Cycles* **14**: 1231–1246.

Luz B, Barkan E. 2000. Assessment of oceanic productivity with the triple-isotope composition of dissolved oxygen. *Science* **288**: 2028–2031.

Marra J. 2007. Approaches to the measurement of plankton production. In: Williams PJlB, Thomas DN, Reynolds CS, eds. *Phytoplankton productivity: carbon assimilation in marine and freshwater ecosystems*. Oxford, UK: Blackwell Science Ltd, 78–108.

Meredith MP, King JC. 2005. Rapid climate change in the ocean west of the Antarctic Peninsula during the second half of the 20th century. *Geophysical Research Letters* **32**: L19604.

Mock T, Hoch N. 2005. Long-term temperature acclimation of photosynthesis in steady-state cultures of the polar diatom Fragilariopsis cylindrus. *Photosynthesis Research* **85**: 307–317.

Moline MA, Prezelin BB. 1996. High-resolution time-series data for 1991/1992 primary production and related parameters at a Palmer LTER coastal site: implications for modeling carbon fixation in the Southern Ocean. *Polar Biology* **17**: 39–53.

Montes-Hugo M, Doney SC, Ducklow HW, Fraser W, Martinson D, Stammerjohn SE, Schofield O. 2009. Recent changes in phytoplankton communities associated with rapid regional climate change along the Western Antarctic Peninsula. *Science* **323**: 1470–1473.

Morgan-Kiss RM, Ivanov AG, Huner NP. 2002. The Antarctic psychrophile, *Chlamydomonas subcaudata*, is deficient in state I–state II transitions. *Planta* **214**: 435–445.

Morgan-Kiss RM, Priscu JC, Pocock T, Gudynaite-Savitch L, Huner NP. 2006. Adaptation and acclimation of photosynthetic microorganisms to permanently cold environments. *Microbiology and Molecular Biology Reviews* **70**: 222–252.

Napolitano MJ, Shain DH. 2005. Quantitating adenylate nucleotides in diverse organisms. *Journal of biochemical and biophysical methods* **63**: 69–77.

Padilla-Gamino JL, Carpenter RC. 2007. Seasonal acclimatization of *Asparagopsis taxiformis* (Rhodophyta) from different biogeographic regions. *Limnology and oceanography* **52**: 833–842.

Parry ML. 2007. *Climate Change 2007: impacts, adaptation and vulnerability: contribution of Working Group II to the fourth assessment report of the Intergovernmental Panel on Climate Change.*, Cambridge, UK and New York, NY, USA: Cambridge University Press.

Pinckney J, Paerl H, Harrington M, Howe K. 1998. Annual cycles of phytoplankton community-structure and bloom dynamics in the Neuse River Estuary, North Carolina. *Marine biology* **131**: 371–381.

Prokopenko MG, Pauluis OM, Granger J, Yeung LY. 2011. Exact evaluation of gross photosynthetic production from the oxygen triple-isotope composition of O2: implications for the net-to-gross primary production ratios. *Geophysical Research Letters* **38**: L14603.

Quay P, Stutsman J, Steinhoff T. 2012. Primary production and carbon export rates across the subpolar N. Atlantic Ocean basin based on triple oxygen isotope and dissolved O2 and Ar gas measurements. *Global Biogeochemical Cycles* **26**: GB2003.

Regaudie-de-Gioux A, Duarte CM. 2012. Temperature dependence of planktonic metabolism in the ocean. *Global Biogeochemical Cycles* **26**: GB1015.

Reuer MK, Barnett BA, Bender ML, Falkowski PG, Hendricks MB. 2007. New estimates of Southern Ocean biological production rates from O_2/Ar ratios and the triple isotope composition of O_2. *Deep Sea Research Part I: Oceanographic Research Papers* **54**: 951–974.

Robinson C, Tilstone GH, Rees AP, Smyth TJ, Fishwick JR, Tarran GA, Luz B, Barkan E, David E. 2009. Comparison of i*n vitro* and *in situ* plankton production determinations. *Aquatic microbial ecology* **54**: 13–34.

Staehr PA, Birkeland MJ. 2006. Temperature acclimation of growth, photosynthesis and respiration in two mesophilic phytoplankton species. *Phycologia* **45**: 648–656.

Sunda WG, Price NM, Morel FM. 2005. Trace metal ion buffers and their use in culture studies. In: Anderson RA, ed. *Algal culturing techniques*. New York, NY, USA: Elsevier Academic Press, 35–63.

Tcherkez GG, Farquhar GD, Andrews TJ. 2006. Despite slow catalysis and confused substrate specificity, all ribulose bisphosphate carboxylases may be nearly perfectly optimized. *Proceedings of the National Academy of Sciences, USA* **103**: 7246–7251.

Tortell PD, Asher EC, Ducklow HW, Goldman JA, Dacey JW, Grzymski JJ, Young JN, Kranz SA, Bernard KS, Morel FM. 2014. Metabolic balance of coastal Antarctic waters revealed by autonomous pCO_2 and ΔO_2/Ar measurements. *Geophysical Research Letters* **41**. doi: 10.1002/2014GL061266.

Valentini R, Matteucci G, Dolman A, Schulze E-D, Rebmann C, Moors E, Granier A, Gross P, Jensen N, Pilegaard K. 2000. Respiration as the main determinant of carbon balance in European forests. *Nature* **404**: 861–865.

Wanninkhof R. 1992. Relationship between wind speed and gas exchange over the ocean. *Journal of Geophysical Research: Oceans (1978–2012)* **97**: 7373–7382.

Welschmeyer NA. 1994. Fluorometric analysis of chlorophyll a in the presence of chlorophyll b and pheopigments. *Limnology and Oceanography* **39**: 1985–1992.

Westwood KJ, Brian Griffiths F, Meiners KM, Williams GD. 2010. Primary productivity off the Antarctic coast from 30°–80° E; BROKE-West survey, 2006. *Deep Sea Research Part II: Topical Studies in Oceanography* **57**: 794–814.

Young JN, Goldman JAL, Kranz SA, Tortell PD, Morel FMM. 2014. Slow carboxylation of Rubisco constrains the maximum rate of carbon fixation during Antarctic phytoplankton blooms. *New Phytologist* **205**: 172–181.

Yvon-Durocher G, Caffrey JM, Cescatti A, Dossena M, del Giorgio P, Gasol JM, Montoya JM, Pumpanen J, Staehr PA, Trimmer M. 2012. Reconciling the temperature dependence of respiration across timescales and ecosystem types. *Nature* **487**: 472–476.

Supporting Information

Additional supporting information may be found in the online version of this article.

Fig. S1 Map of the sampling region around Palmer station.

Fig. S2 Depth profiles of temperature, salinity and density at LTER-station B.

Fig. S3 Mixed layer depths throughout the season determined by density profiles.

Fig. S4 Concentrations of major nutrients throughout the season (CO_2 in µmol kg SW^{-1} and NO_3^-, SiO_2, PO_4^{3-} in µmol l^{-1}).

Fig. S5 Chlorophyll a normalized gross photosynthesis (as measured with ^{18}O incubations) vs the average PAR during the incubation.

Fig. S6 Bacterial respiration during the season (10-m depth, LTER – station B) measured with thymidine incorporation.

Notes S1 ^{14}C net primary production – correction for the respiration (R) of the unlabelled carbon during the 24 h incubations.

Notes S2 Determining GPP and NCP rates from triple oxygen isotope and dO_2/Ar.

Notes S3 Electron flow measurements – correction of the artefact.

Notes S4 Bacteria productivity – thymidine measurements.

Table S1 Summary of data from incubations with $H_2{}^{18}O$

Table S2 Summary of data to estimate Gross and Net production from dO_2/Ar and triple isotope composition

Table S3 Nonsteady-states rates of Gross and Net community production assuming the samples are below or above the mixed layer

Please note: Wiley Blackwell are not responsible for the content or functionality of any supporting information supplied by the authors. Any queries (other than missing material) should be directed to the *New Phytologist* Central Office.